HOKKAIDO UNIVERSITY

Title	Shear-Thinning Characteristics of Nematic Liquid Crystals Doped with Nanoparticles
Author(s)	Kimura, Munehiro; Hanafi, Zur Ain Binti; Takagi, Tatsuya et al.
Citation	Crystals, 6(11), 145 https://doi.org/10.3390/cryst6110145
Issue Date	2016-11
Doc URL	https://hdl.handle.net/2115/64488
Rights(URL)	https://creativecommons.org/licenses/by/4.0/
Type	journal article
File Information	crystals-06-00145.pdf

Hokkaido University Collection of Scholarly and Academic Papers : HUSCAP

crystals

MDPI

Article

Shear-Thinning Characteristics of Nematic Liquid Crystals Doped with Nanoparticles

Munehiro Kimura [1,*], Zur Ain Binti Hanafi [1], Tatsuya Takagi [1], Ryosuke Sawara [1] and Shuji Fujii [2]

[1] Department of Electrical Engineering, Graduate School of Engineering, Nagaoka University of Technology, 1603-1 Kamitomioka, Nagaoka, 940-2188 Niigata, Japan; zurain1115@gmail.com (Z.A.B.H.); s121051@stn.nagaokaut.ac.jp (T.T.); s153149@stn.nagaokaut.ac.jp (R.S.)

[2] Department of Applied Physics, Graduate School of Engineering, Hokkaido University, 060-8628 Sapporo, Japan; sfujii@eng.hokudai.ac.jp

* Correspondence: nutkim@vos.nagaokaut.ac.jp; Tel.: +81-258-47-9540; Fax: +81-258-47-9500

Academic Editor: Charles Rosenblatt

Received: 15 September 2016; Accepted: 9 November 2016; Published: 12 November 2016

Abstract: This work investigated changes in the physical properties of nematic liquid crystals (NLCs) upon doping with nanoparticles. Shear viscosity measurements demonstrated the shear-thinning of typical NLCs following the addition of small amounts of nanoparticles at approximately 1 wt. %. However, neither the birefringence nor the dielectric anisotropy was significantly affected at these levels of doping. The shear-thinning appears to result from the locally ordered alignment of the NLCs in the vicinity of the nanoparticles rather than from reductions in the bulk order parameters.

Keywords: nematic liquid crystals; nanoparticles; shear-thinning; order parameter; birefringence

1. Introduction

The rheological properties of liquid crystals (LCs) remain a topic of significant interest, both from scientific and practical points of view. As an example, demands for high-definition television monitors have accelerated the development of LC compounds for use in liquid crystal displays (LCDs). Novel LC molecules have been synthesized, and the properties of these compounds have been elucidated [1]. A simple means of improving the response speed of an LCD is to reduce the viscosity of the LC compound on which it is based [2], so several LC homologues have been made for this purpose. Recently, Kobayashi's group proposed another method of increasing the response speed based on the addition of nanoparticles [3]. Doping with nanoparticles in this manner is thought to improve response speeds by reducing the order parameter of nematic LCs (NLCs) [4]. There have been various other reports regarding the physical characteristics of nanoparticle-doped LCs. One study demonstrated that adding colloidal particles effectively improved the physical properties of the host NLC. Spherical colloidal particles with lengths on the mesoscopic scale have been found to distort the alignment of the LC as the result of interactions between the particles [5–7]. Semiconductor nanorods have been used to enhance the re-orientational effect in LCs as well as to tune the refractive index of these materials [8]. More recently, ferroelectric nanoparticles have attracted significant attention with regard to controlling the responses of NLC molecules. The ferroelectric nature of these nanoparticles can greatly enhance the physical and electro-optic properties of the host LC, including its phase transition temperature, dielectric and optical anisotropy, and Fréedericksz transition [9–14]. In a ferroelectric nanoparticle-doped system, the nanoparticles behave as molecular dipoles and can therefore affect the resulting LC order. The functioning of these ferroelectric nanoparticles has been intensively studied, although the geometrical effect of doping with nanoparticles having lengths in the range of 10–100 nm on the alignment of LC molecules is

still unknown. Nanoparticles with such small dimensions are expected to have a minimal distortion effect on the LC matrix, and instead may function as impurities that affect the physical properties of the host LC.

Another requirement associated with the fabrication of electronic displays is a low production cost. Kimura et al. recently proposed a technique known as the slit coater method as a novel fabrication process for LCDs [15–17]. It is known that the viscoelasticity of LCs is associated with the self-organization of LC layers. It has also been shown that, when an LC compound is coated onto a substrate, the flow-induced shear between the nozzle and the substrate regulates the LC molecular alignment. An outstanding feature of the slit coater method is that a conventional alignment film is unnecessary, making this technique applicable to the manufacture of flexible LCDs by substituting a plastic substrate for the conventional glass substrate. Although the mechanism by which LC molecules are regulated is still not fully understood, it is assumed that the viscosity of the LC compound is an important factor [18]. Numerical simulations of flow alignment have been demonstrated based on classical tensor order parameter equations [19]; however, neither three-dimensional calculations nor simulations that take into account all the individual molecular characteristics have yet been explored.

As noted, adding various dopants into an LC host compound is one simple means of controlling the viscosity, and inorganic nanoparticles acting as viscosity reducers and/or thickeners may be useful in this regard because of their lack of reactivity with LCs. In the present study, LCD cells were fabricated using the slit coater method in conjunction with nanoparticle-doped NLCs. The viscosity of each NLC both with and without nanoparticles, a property that plays an important role during slit coating, was investigated by employing a rheometer. In addition, the effects of doping on both the dielectric anisotropy and birefringence of each LC were assessed. Herein, we present a hypothesis as to why doping with silica nanoparticles affects solely the LC viscosity.

2. Nanoparticle-Doped NLCs

MLC-14100-000 (Merck, Kanagawa, Japan) was used as the host NLC to investigate the applicability of the slit coater method in association with nanoparticle doping. MLC-14100 is a mixture of fluorinated biphenyl compounds, and was employed because its viscosity and elastic constant are similar to those of the simpler NLC material ZLI-2293 (Merck, Kanagawa, Japan) used in our previous studies [15–17]. NTN-02 and NTN-03 (DIC Co., Saitama, Japan) were employed as the NLCs in the viscosity measurements. These compounds were originally prepared for applications in active and passive LCDs, respectively. As a first step, the principal physical parameters of these NLCs were determined. These are listed in Table 1, where K_{11} and K_{33} are the splay and bend elastic constants, $\varepsilon_{//}$ and $\varepsilon_{\perp}$ are the dielectric constant parallel and perpendicular to the long molecular axis, and n_o and n_e are the refractive indices in the case of ordinary and extraordinary light beams, respectively. For reasons related to intellectual property, there is very limited information available regarding the compositions of NTN-02 and NTN-03. It is known that these are mixtures of fluorinated biphenyls and that the purity of each NLC mixture is suitably high, giving a resistivity of more than 10 MΩ·cm. Both a 7 nm spherical silica (Aerosil R-812, Evonik, Essen, Germany) and a 40 nm spherical silica (RX-50, Nippon Aerosil Co., Yokkaichi, Japan) were employed as the nanoparticle dopants and were added at a concentration of 1.0 wt. %. The surfaces of the as-received R-812 and RX-50 were covered with thin hydrophobic overcoats of hexamethyldisilazane to prevent aggregation. Previously, decreases in threshold voltage have been confirmed when using NTN-02 with R-812 [3], and we propose that this occurs because the bulk order parameter is decreased by the addition of the nanoparticles. This means that the threshold voltage and rotational viscosity are also reduced. Hakobyan et al. have reported that the change in the bulk order parameter can be estimated in the case that the host NLC is achiral [11]. Kobayashi's paper also stresses that the use of chiral dopants in NLCs plays an important role in the dispersion of the nanoparticles [3]. In our work, the NTN-02 and NTN-03 both contained small amounts of a chiral dopant, with a nominal chiral pitch of 12 μm at 25 °C. In the case of cholesteric liquid crystals (or chiral-doped NLCs) it is virtually

impossible to evaluate the bulk order parameter and elastic constant directly so long as the NLC mixture contains a chiral dopant. In contrast, it is also well known that both birefringence and dielectric anisotropy depend on the bulk order parameter [11,20]. In the present study, the viscosity, birefringence, dielectric anisotropy, and threshold voltage of NTN-03, with and without doping nanoparticles, were investigated. The change in the bulk order parameter was subsequently estimated from the differences in the birefringence and dielectric anisotropy before and after the addition of the nanoparticles.

Table 1. Principal physical parameters of the NLCs used in this work.

	NTN-02	**NTN-03**	
K_{11}	9.14 pN	7.60 pN	
K_{33}	8.45 pN	8.11 pN	
$\varepsilon_{//}$	7.60	8.76	@ 1 kHz
$\varepsilon_{\perp}$	2.86	3.23	
n_e	1.625	1.623	@ 589.3 nm
n_o	1.499	1.496	

3. Experimental

The slit coater experiments were carried out using an instrument of our own design [15–17], as shown in Figure 1. The slit width, slit length, and gap between the slit nozzle and the substrate were fixed at 20 μm, 13 mm, and approximately 100 μm, respectively. The substrate was moved at 0.5 mm/s. These coating conditions appear to be optimal when working with NLCs with viscosity values in the vicinity of 100 mPa·s.

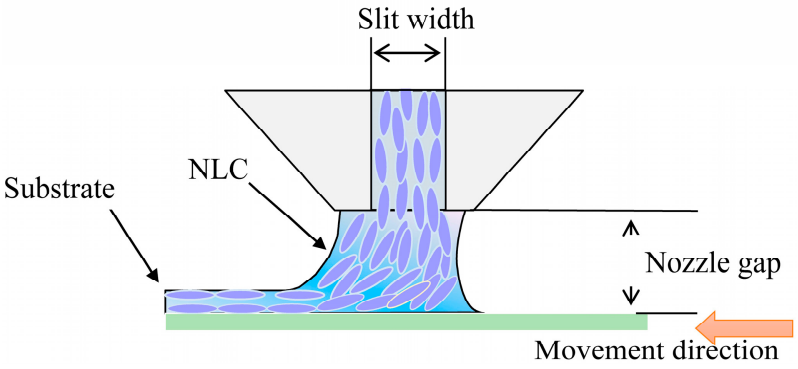

Figure 1. Schematic diagram of the slit coater.

Rheological measurements were also performed in this study and information regarding the bulk viscosity was used to quantify the effect of the nanoparticles. Viscosity data were acquired with an ARES-G2 strain-controlled rheometer (TA Instrument Co. Ltd., New Castle, DE, USA) in conjunction with a cone and plate shear cell (cone diameter = 40 mm, angle = 0.04 rad). Prior to these measurements, we applied a pre-shear of 500 s^{-1} for 100 s to each specimen to ensure homogeneous dispersion of the nanoparticles. During viscosity measurements, shear rates ranging from 10–500 s^{-1} were applied in a stepwise manner, over 1800 s. We confirmed the reproducibility of the viscosity data by repeating the same measurements twice. The shear viscosity was measured at 25 °C.

The dielectric constant, threshold voltage, and elastic constant were determined using a conventional sandwich-type LCD cell, whose inner surfaces were covered with an LC alignment film made of polyimide (JNC Petrochemical Corp., Ichihara, Japan), subjected to a moderate degree of rubbing. The rubbing direction was antiparallel in the conventional electrically controlled birefringence (ECB) mode and perpendicular in the conventional twisted nematic (TN) mode. The gap between

the two glass substrates was 4 μm and, as a result of the small amount of chiral dopant mixed with the nanoparticles, the chiral pitch was 12 μm at 25 °C. The NLC sample with added nanoparticles was mixed for more than 5 h in an ultrasonic mixer at approximately 100 °C prior to analysis. Subsequently, to ensure that the nanoparticles were homogeneously dispersed throughout the host matrix, the NLC/nanocomposite combination was agitated for several minutes using a vortex mixer. Following this, the specimen was transferred to the sandwich cell in an isotropic phase. The sample was cooled to 25 °C before conducting experimental measurements. Anisotropic dielectric constants parallel and perpendicular to the long molecular axis were obtained by means of a capacitance meter (EC-1, Toyo Co., Tokyo, Japan) while applying an external voltage. Using the ECB cell, $\varepsilon_{//}$ and $\varepsilon_{\perp}$ values, as well as the threshold voltage, could be determined based on the dependence of the ECB cell capacitance on the applied voltage (the so-called C-V method). Anisotropic refractive indices were evaluated using transmission ellipsometry (M-150, JASCO, Hachioji, Japan). Based on plural incidence renormalized transmission spectroscopic ellipsometry, the wavelength dispersion associated with birefringence was assessed using both the TN and ECB cells. Details of these measurement procedures have been provided in a previous paper [21]. The LC texture was examined by crossed nicols polarizing optical microscopy (POM, Eclipse LV100 POL, Nikon, Tokyo, Japan).

4. Results and Discussion

It would, of course, be desirable to improve the LC alignment simply by doping with nanoparticles. In our initial experiments, the purpose was therefore to ascertain the applicability of nanoparticle doping to the slit coater method. Figure 2 presents microphotographs of the NLC alignment obtained when using the slit coater with the MLC-14100-000 as the host NLC, with a nominal LC layer thickness of 2 μm. In the absence of R-812 doping, uniform alignment of the NLC molecules was confirmed, as shown in Figure 2a,b. In contrast, the addition of 1 wt. % R-812 resulted in imperfect alignment, as seen in Figure 2c,d. Unexpectedly, even when using the other host materials (NTN-02 or NTN-03), the LC alignment was reduced upon doping with the R-812. From these experimental results, two possible reasons for the observed alignment deterioration can be proposed. One involves sedimentation of the nanoparticles in the vicinity of the substrate after transferring the NLC mixture into the sandwich cell [14]. However, such sedimentation and/or aggregation could not be confirmed in the present work when using a conventional sandwich cell together with the rubbing method. To determine the degree of sedimentation and/or aggregation, more detailed investigations using cryo-electron microscopy will be necessary. Another possible cause is a greater-than-expected viscosity increase, such that the shear force was not well suited to aligning the NLC molecules uniformly. In order to assess the feasibility of the latter hypothesis, viscosity measurements were carried out using a rheometer.

The shear rate dependencies of the viscosity for MLC-14100-000, with and without nanoparticle doping, are shown in Figure 3. In the absence of nanoparticles, the viscosity was almost constant over a wide range of shear rates. This was equivalent to the behavior of a Newtonian fluid, as expected for a low-molecular-weight NLC. Conversely, when R-812 or RX-50 was doped into the host NLC, the viscosity decreased with increases in the shear rate, which is known as shear-thinning and is not observed in Newtonian fluids.

Figure 4a,b present the viscosity as a function of the shear rate for two host NLCs, NTN-02 and NTN-03, with and without nanoparticle doping. It is obvious that the shear-thinning viscosity is observed for doped systems with either R-812 or RX-50, while a weak shear-thinning effect can be observed in the case of the NTN-02 without doping. In Figure 4b, adding chiral dopant also slightly increases the viscosity. However, adding nanoparticles increases the viscosity more effectively. These data also show that smaller nanoparticles led to higher viscosity, which suggests that the alignment of NLCs around the nanoparticles affects such rheological behavior.

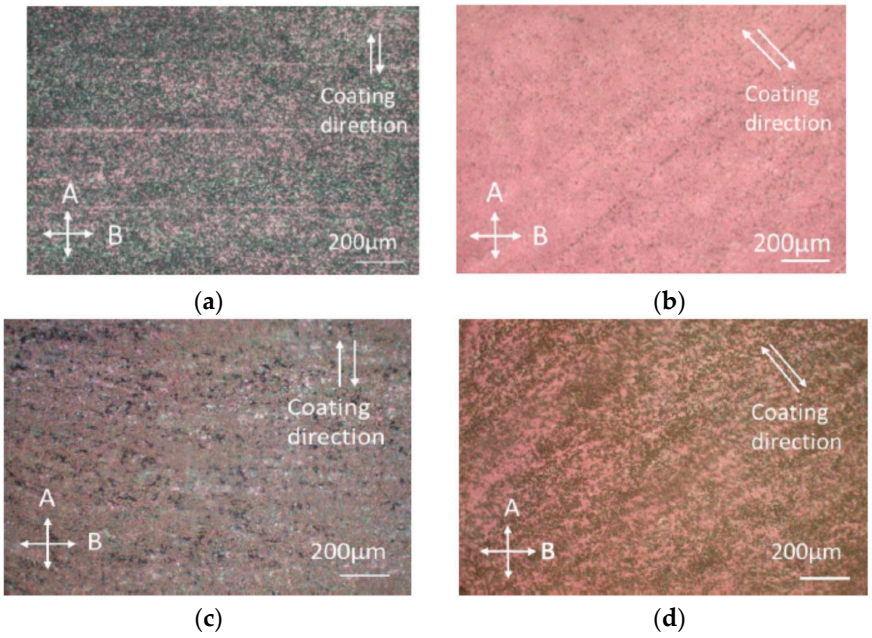

Figure 2. Microphotographs taken after slit coating. Host NLC used was MLC-14100-000: (**a**) without doping and with the coating direction parallel to the analyzer; (**b**) without doping and with the coating direction 45° with respect to the analyzer; (**c**) with nanoparticle doping and the coating direction parallel to the analyzer; and (**d**) with nanoparticle doping and the coating direction 45° with respect to the analyzer.

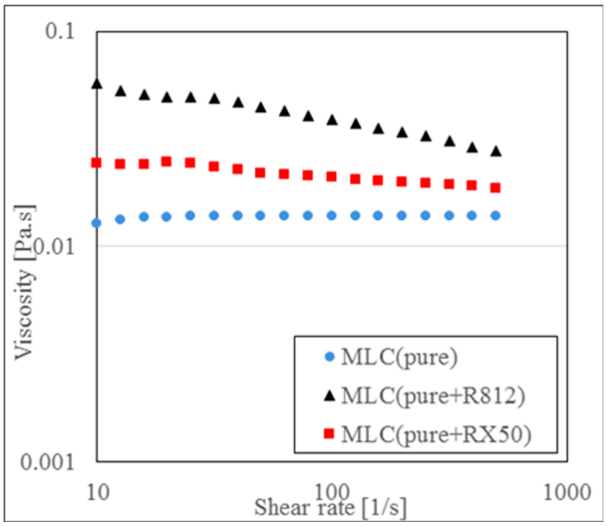

Figure 3. The shear rate dependence of the viscosity for MLC-14100-000 systems with and without nanoparticles, R812 and RX50.

It is known that both birefringence and the dielectric constant depend on the bulk order parameter. Thus, to estimate the effect of nanoparticle doping on the bulk order parameter, the birefringence and dielectric constant, with and without doping nanoparticles, were investigated. It should be noted that the sample cell filled with pure NTN-03 was in the planar (antiparallel) configuration, while the sandwich cell injected with NTN-03 doped with R-812 was in the TN configuration. This occurred because adding small amounts of the chiral dopant improved the dispersion of the nanoparticles. As a result of this effect, the nominal chiral pitch of the sample was 12 μm and the cell gap was 3 μm. Because of the differences in these sample configurations, it was not

possible to determine the elastic constants. Figure 5 shows the birefringence wavelength dispersion, Δn, of the NTN-03 with and without doping with R-812. Here, a very simple Cauchy dispersion and a similar dependence of Δn are evident. These experimental results suggest that the birefringence is only very slightly affected by doping. Figure 6 summarizes the dependence of the capacitance on the applied voltage, using NTN-03. The experimental capacitance values plotted here have been normalized by the capacitance result obtained when no electric voltage was applied to the sample (that is, by C_0). As shown in Figure 6, the application of a high electric voltage to the samples caused the normalized capacitances to approach plateaus, although the two materials generated different plots. Both $\varepsilon_{//}$ and $\varepsilon_{\perp}$ can be readily calculated from these data using the values for the cell gap and the electrode area. These calculations showed that the addition of nanoparticles made no difference to Δε. As shown in Figure 6b, the threshold voltage was almost the same in both cases. This result implies that the bulk order parameter was not significantly affected by the nanoparticles up to the maximum concentration of 1 wt. %. Unlike their effect on viscosity, the effects of the doped nanoparticles appear to be spatially restricted in these experimental results, since both the dielectric constant and refractive index are static and volume-integral parameters.

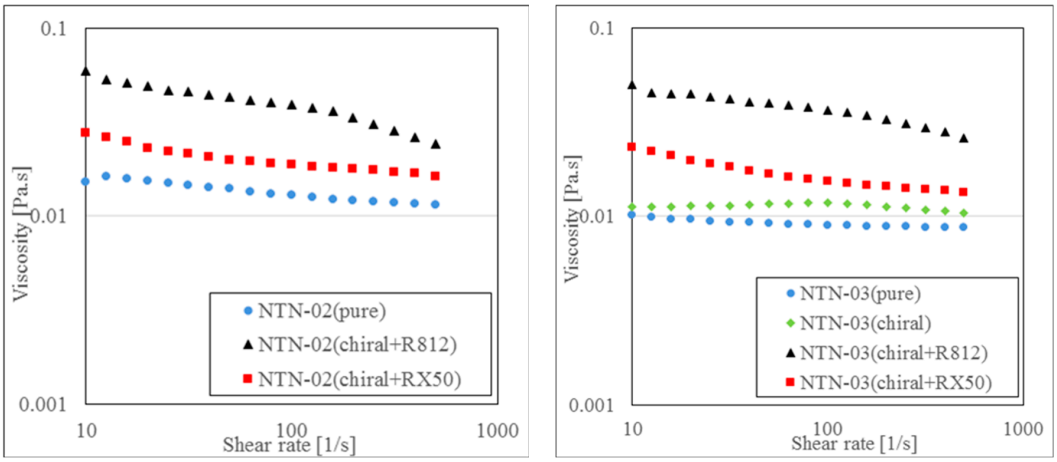

Figure 4. The shear rate dependence of the viscosity for NTN-02 (**a**) and NTN-03 (**b**) with and without nanoparticles, R812 and RX50.

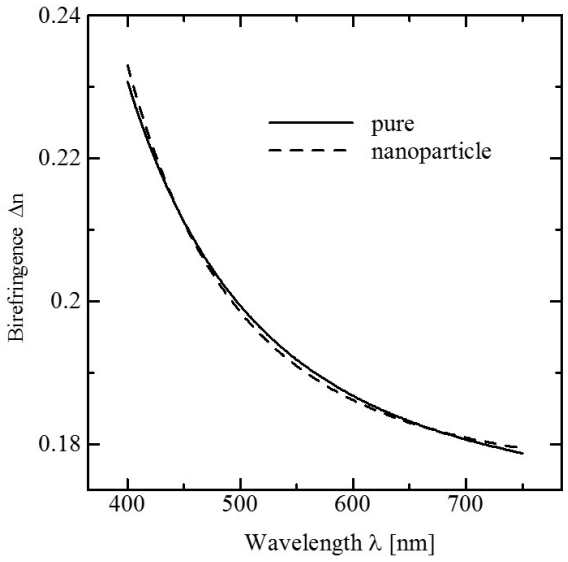

Figure 5. Birefringence wavelength dispersion values, Δn, with and without doping with R-812.

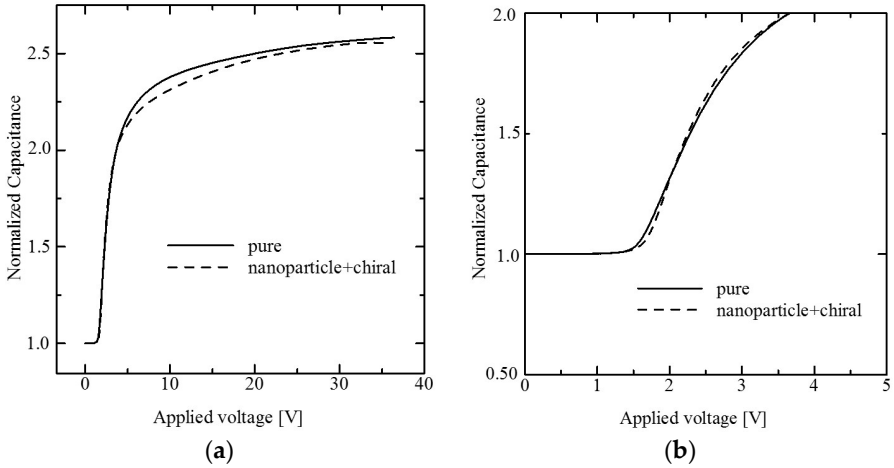

Figure 6. (**a**) Dependence of the normalized NLC cell capacitance on the applied voltage with and without doping with R-812 and (**b**) enlarged view of the region of (**a**) around the threshold voltage.

At this point, it is helpful to assess the effects of size on the shear-thinning phenomenon induced by the nanoparticles. To simplify the investigation, we focused on a single nanoparticle and the surrounding NLC molecular alignment, even though the matrix consisting of the nanoparticles and NLC might actually represent a colloidal system. It is likely that the NLC molecules tended to align radially against the nanoparticles [22], because the surfaces of the nanoparticles were covered by a hydrophobic overcoat of the surfactant. In the case of a conventional sandwich-type cell, it is well known that the NLCs prefer to align perpendicular to the hydrophobic surface. Based on the same analogy, the NLC molecular alignment in the vicinity of the nanoparticles will be controlled by the characteristics of the nanoparticles, such that the NLC will tend to align parallel to the surface normal of each nanoparticle rather than along the surface, as illustrated in Figure 7a. This proposed alignment is similar to that reported for colloidal systems and/or ferroelectric nanoparticles [5–14]. Here, we can compare the effects of doping with the two sizes of nanoparticles: R-812 (7 nm) and RX-50 (40 nm). Adding the same weight percentages of nanoparticles to the NLCs will generate different values for the effective nanoparticle surface area (that is, the surface area over which the NLC molecules make contact). Specifically, even when the same weight and volume of nanoparticles are doped into a unit volume of the host NLC, the greater size of the RX-50 particles (approximately six times that of the R-812) results in a greater number of R-812 particles, by a factor of approximately 6^3. The surface area of an RX-50 particle is 6^2 times that of an R-812 particle, so the total surface area of the R-812 will be six times larger than that of the RX-50. Figure 7c presents an exaggerated illustration of the NLC molecular alignment around the nanoparticles, showing a transverse section in which the circle represents the surface of a nanoparticle. Both the R-812 and RX-50 particles are silica, which is not ferroelectric, but rather dielectric. For this reason, it is believed that the NLCs will be oriented around the nanoparticle based on intermolecular interactions between the NLCs and the surfactant on the nanoparticle surfaces, rather than as a result of Coulomb forces [22]. Despite this, the aspect of the NLC alignment will be similar to that generated when using ferroelectric nanoparticles [12]. To simplify these hypotheses, neither aggregation nor sedimentation effects are taken into account. It is obvious that larger nanoparticles will have greater surface areas, and it is assumed that increases in the effective surface area (that is, the area over which there is contact between the nanoparticles and the NLC molecules) increase the attractive force between the nanoparticles and the NLC molecules originating from intermolecular interactions. Based on a simple estimation, in the case of the R-812, the effective surface anchoring energy per unit volume of the host NLC will be six times greater than that of the RX-50. This pseudo-surface anchoring between the nanoparticles and host NLC molecules would be expected to increase the viscosity. The shear rate variations are not as easy to interpret,

although the shear-thinning behavior of bent-core liquid crystals has been reported by Bailey et al. [23], who proposed the existence of nanostructured, fluctuating clusters composed of a few smectic-like layers. Our data suggest that similar nanostructures may have formed around the doped nanoparticles and that these could be the cause of the shear-thinning behavior.

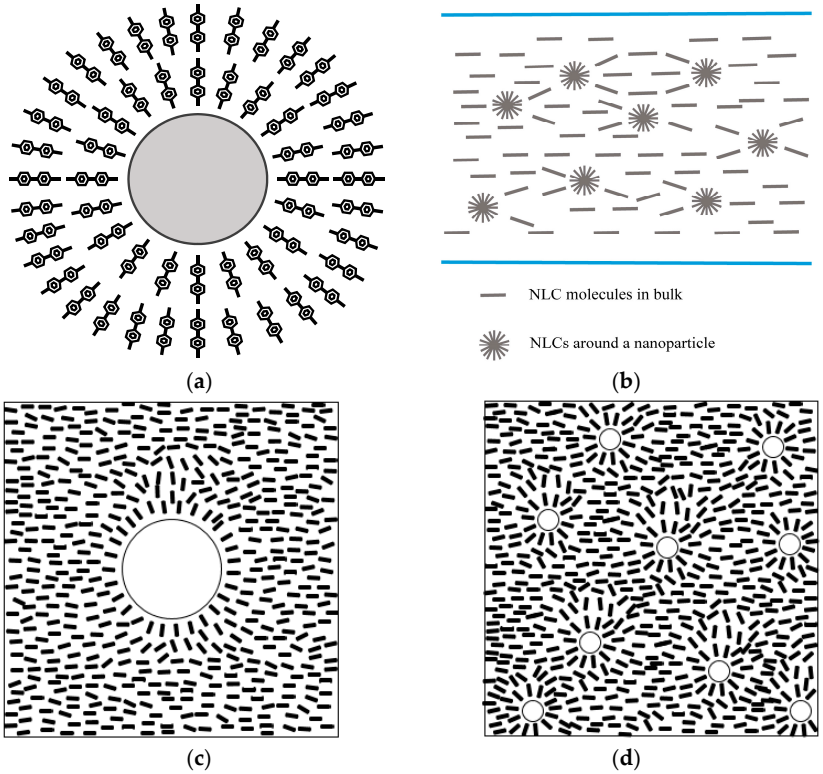

Figure 7. (**a**) NLC alignment around a single nanoparticle; (**b**) the bulk NLC/nanoparticle mixture; (**c**) NLC alignment around a 40 nm RX-50 nanoparticle; and (**d**) NLC alignment around 7 nm R-812 nanoparticles, applying the same mass of nanoparticles as in the case of (**c**).

5. Conclusions

This work investigated changes in the physical properties of NLCs upon doping with nanoparticles. Shear viscosity measurements showed that shear-thinning behavior was induced in conventional NLCs following the addition of small amounts of nanoparticles (1 wt. %). In contrast, there was little effect on either the birefringence or dielectric anisotropy. The observed shear-thinning likely results from locally ordered NLC alignment in the vicinity of the nanoparticles as opposed to a reduction in the bulk order parameter.

Acknowledgments: This work was supported by a JSPS Grant-in-Aid for Scientific Research (C) (No. 25390053). The authors wish to express their appreciation to Shunsuke Kobayashi (Tokyo University of Science) for fruitful discussions and for encouraging this study. The authors thank the DIC Co. and Merck for providing LC samples, and the Nippon Aerosil Co. Ltd. for supplying nanoparticles.

Author Contributions: Munehiro Kimura conceived and designed the experiments; Zur Ain Binti Hanafi, Tatsuya Takagi and Ryosuke Sawara performed the experiments; Shuji Fujii analyzed the viscosity data; Munehiro Kimura wrote the paper.

Conflicts of Interest: The authors declare no conflict of interest.

References

1. Bremer, M.; Kirsch, P.; Klasen-Memmer, M.; Tarumi, K. The TV in your pocket: Development of liquid-crystal materials for the new millennium. *Angew. Chem. Int. Ed.* **2013**, *52*, 8880–8896. [CrossRef] [PubMed]

2. Chen, H.; Hu, M.; Peng, F.; Li, J.; An, Z.; Wu, S.T. Ultra-low viscosity liquid crystal materials. *Opt. Mater. Express* **2015**, *5*, 655–660. [CrossRef]
3. Kobayashi, S.; Akimoto, M.; Takatoh, K.; Shiraishi, Y.; Sawai, H.; Toshima, N.; Takeuchi, K.; Kotani, K.; Kaneoya, M.; Takeishi, K.; et al. Electro-optical properties of LCD doped with nanoparticles and with optical compensators: Way for fast response. *Mol. Cryst. Liq. Cryst.* **2014**, *594*, 21–30. [CrossRef]
4. Zakerhamidi, M.S.; Shoarinejad, S.; Mohammadpour, S. Fe_3O_4 nanoparticle effect on dielectric and ordering behavior of nematic liquid crystal host. *J. Mol. Liq.* **2014**, *191*, 16–19. [CrossRef]
5. Poulin, P.; Stark, H.; Lubensky, T.C.; Weitz, D.A. Novel colloidal interactions in anisotropic fluids. *Science* **1997**, *275*, 1770–1773. [CrossRef] [PubMed]
6. Smalyukh, I.I.; Lavrentovich, O.D.; Kuzmin, A.N.; Kachynski, A.V.; Prasad, P.N. Elasticity-mediated self-organization and colloidal interactions of solid spheres with tangential anchoring in a nematic liquid crystal. *Phys. Rev. Lett.* **2005**, *95*, 157801. [CrossRef] [PubMed]
7. Muševič, I.; Škarabot, M.; Tkalec, U.; Ravnik, M.; Žumer, S. Two-dimensional nematic colloidal crystals self-assembled by topological defects. *Science* **2006**, *313*, 954–958. [CrossRef] [PubMed]
8. Khoo, I.-C.; Chen, K.; Williams, Y.Z. Orientational photorefractive effect in undoped and CdSe nanorods-doped nematic liquid crystal—Bulk and interface contributions. *IEEE J. Sel. Top. Quantum Electron.* **2006**, *12*, 443–450. [CrossRef]
9. Kaczmarek, M.; Buchnev, O.; Nandhakumar, I. Ferroelectric nanoparticles in low refractive index liquid crystals for strong electrooptic response. *Appl. Phys. Lett.* **2008**, *92*, 103307. [CrossRef]
10. Lopatina, L.M.; Selinger, J.V. Maier-Saupe-type theory of ferroelectric nanoparticles in nematic liquid crystals. *Phys. Rev. E* **2011**, *84*, 041703. [CrossRef] [PubMed]
11. Hakobyan, M.R.; Alaverdyan, R.B.; Hakobyan, R.S.; Chilingaryan, Y.S. Enhanced physical properties of nematics doped with ferroelectric nanoparticles. *Armen. J. Phys.* **2014**, *7*, 11–18.
12. Basu, R. Soft memory in a ferroelectric nanoparticle-doped liquid crystal. *Phys. Rev. E* **2014**, *89*, 022508. [CrossRef] [PubMed]
13. Podoliak, N.; Buchnev, O.; Herrington, M.; Mavrona, E.; Kaczmarek, M.; Kanaras, A.G.; Stratakis, E.; Blach, J.-F.; Henninot, J.-F.; Warenghem, M. Elastic constants, viscosity and response time in nematic liquid crystals doped with ferroelectric nanoparticles. *RSC Adv.* **2014**, *4*, 46068–46074. [CrossRef]
14. Urbanski, M. On the impact of nanoparticle doping on the electro-optic response of nematic hosts. *Liq. Crys. Today* **2015**, *24*, 102–115. [CrossRef]
15. Sato, H.; Miyashita, K.; Kimura, M.; Akahane, T. Study of liquid crystal alignment formed using slit coater. *Jpn. J. Appl. Phys.* **2011**, *50*, 01BC16. [CrossRef]
16. Kimura, M.; Yodogawa, S.; Ohtsuka, K.; Yatsushiro, T.; Hirata, H.; Akahane, T. Flexible LCDs fabricated with a slit coater. *J. Soc. Inf. Disp.* **2012**, *20*, 633–639. [CrossRef]
17. Kimura, M.; Nagataki, Y.; Ueda, K.; Yamamoto, T. Study on the functions of UV curable reactive mesogen in LCDs fabricated by coating method. *J. Photopolym. Sci. Technol.* **2014**, *27*, 291–296. [CrossRef]
18. Mather, P.T.; Pearson, D.S.; Larson, R.G. Flow patterns and disclination-density measurements in sheared nematic liquid crystals I: Flow-aligning 5CB. *Liq. Cryst.* **1996**, *20*, 527–538. [CrossRef]
19. Grecov, D.; Rey, A.D. Texture control strategies for flow-aligning liquid crystal polymers. *J. Non-Newton. Fluid Mech.* **2006**, *139*, 197–208. [CrossRef]
20. De Gennes, P.G.; Prost, J. *The Physics of Liquid Crystals*, 2nd ed.; Oxford University Press: New York, NY, USA, 1993; pp. 59–60.
21. Goda, K.; Kimura, M.; Akahane, T. Improved method for the dispersion of refractive indices based on transmission spectroscopic ellipsometry. *Mol. Cryst. Liq. Cryst.* **2011**, *545*, 242–248. [CrossRef]
22. Rahimi, M.; Roberts, T.F.; Armas-Pérez, J.C.; Wang, X.; Bukusoglu, E.; Abbott, N.L.; de Pablo, J.J. Nanoparticle self-assembly at the interface of liquid crystal droplets. *Proc. Natl. Acad. Sci. USA* **2015**, *112*, 5297–5302. [CrossRef] [PubMed]
23. Bailey, C.; Fodor-Csorba, K.; Gleeson, J.T.; Sprunt, S.N.; Jakli, A. Rheological properties of bent-core liquid crystals. *Soft Matter* **2009**, *5*, 3618–3622. [CrossRef]

© 2016 by the authors; licensee MDPI, Basel, Switzerland. This article is an open access article distributed under the terms and conditions of the Creative Commons Attribution (CC-BY) license (http://creativecommons.org/licenses/by/4.0/).